remote sensing

MDPI

Article

Mapping *Lantana camara* and *Leucaena leucocephala* in Protected Areas of Pakistan: A Geo-Spatial Approach

Iram M. Iqbal [1,2,*], Heiko Balzter [2,3], Firdaus-e-Bareen [1,4] and Asad Shabbir [1,5]

[1] Ecology and Evolution Lab, Institute of Botany, University of the Punjab, Quaid-e-Azam Campus, Lahore 54590, Pakistan
[2] School of Geography, Geology and the Environment, Institute for Environmental Futures, University of Leicester, Space Park Leicester, 92 Corporation Road, Leicester LE4 5SP, UK
[3] National Centre for Earth Observation, University of Leicester, University Road, Leicester LE1 7RH, UK
[4] Institute of Molecular Biology and Biotechnology, University of Lahore, Lahore 54000, Pakistan
[5] Weeds Biosecurity, New South Wales Department of Primary Industries, Orange, NSW 2800, Australia
* Correspondence: irammujahid.botany@pu.edu.pk

Abstract: Invasive alien plants are considered as one of the major causes of loss of native biodiversity around the world. Remote sensing provides an opportunity to identify and map native and invasive species using accurate spectral information. The current study was aimed to evaluate PlanetScope (3 m) and Sentinel (10 m) datasets for mapping the distribution of native and invasive species in two protected areas in Pakistan, using machine learning (ML) algorithms. The multispectral data were analysed with the following four ML algorithms (classifiers)—random forest (RF), Gaussian mixture model (GMM), k-nearest neighbour (KNN), and support vector machine (SVM)—to classify two invasive species, *Lantana camara* L. (common lantana) and *Leucaena leucocephala* L. The (Ipil-ipil) Dzetsaka plugin of QGIS was used to map these species using all ML algorithms. RF, GMM, and SVM algorithms were more accurate at detecting both invasive species when using PlanetScope imagery rather than Sentinel. Random forest produced the highest accuracy of 64% using PlanetScope data. *Lantana camara* was the most dominating plant species with 23% cover, represented in all thematic maps. *Leucaena leucocpehala* was represented by 7% cover and was mainly distributed in the southern end of the Jindi Reserve Forest (Jhelum). It was not possible to discriminate native species *Dodonea viscosa* Jacq. (Snatha) using the SVM classifier for Sentinel data. Overall, the accuracy of PlanetScope was slightly better than Sentinel in term of species discrimination. These spectral findings provide a reliable estimation of the current distribution status of invasive species and would be helpful for land managers to prioritize invaded areas for their effective management.

Keywords: discrimination; dzetsaka tool; machine learning; *Leucaena leucocephala*; *Lantana camara*; protected areas

check for updates

Citation: Iqbal, I.M.; Balzter, H.; Firdaus-e-Bareen; Shabbir, A. Mapping *Lantana camara* and *Leucaena leucocephala* in Protected Areas of Pakistan: A Geo-Spatial Approach. *Remote Sens.* **2023**, *15*, 1020. https://doi.org/10.3390/rs15041020

Academic Editor: João Catalão Fernandes

Received: 15 December 2022
Revised: 6 February 2023
Accepted: 7 February 2023
Published: 12 February 2023

Copyright: © 2023 by the authors. Licensee MDPI, Basel, Switzerland. This article is an open access article distributed under the terms and conditions of the Creative Commons Attribution (CC BY) license (https://creativecommons.org/licenses/by/4.0/).

1. Introduction

Invasive alien plants are non-native species that may have negative impacts on native biodiversity, the economy, agricultural productivity, and human and animal health [1]. The traditional field-based survey approaches to document the spread of invasive plants need to be improved [2,3], as accurate spread assessment across large landscapes is a difficult task [4]. Some of the limitations of field-based methods (ecological surveys) include higher costs, time intensiveness, less accessibility of sites, and visual calculation errors [5]. It is critical to explore advanced methods that are accurate and more powerful to document current spread and long-term monitoring of invasive species across the landscape [6,7].

Early detection of invasive plant species using different spatial and temporal monitoring techniques (Geographic Information Systems (GIS) and remote sensing) helps in successful management of these invaders [8–10]. The development of maps showing invasive plants' cover is a reliable method for long term monitoring and implementing effective

control strategies in protected areas [11]. Protected areas are for conserving biodiversity and natural resources around the globe. Remote sensing plays an important role in the unbiased detection and quantification of invasive vegetation cover [12,13]. Studies have shown that each plant species, regardless of its origin (native or introduced), has a unique spectral reflectance due to dissimilar physical and biochemical characteristics that ultimately help species-level identification using remote sensing methods [14]. Different imaging and non-imaging sensors can be used to obtain spectral measurements of plant species, and these data are acquired by a range of airborne and space-borne sensors (multispectral or hyperspectral) with coarse to fine spatial resolutions [15–17]. Most studies involving the use of multispectral satellite sensors to delineate plant species have used different image classification approaches, such as machine learning and pixel-based classification [18,19]. Generally, hyperspectral data identify and discriminate the target species more accurately [20,21], but they are not widely used in research due to the lack of accessibility and high cost. Similarly, high-spatial-resolution sensors have shown better results for detecting vegetation, but often their temporal resolution is low [22]. Therefore, multispectral medium resolution sensors are still considered good for species discrimination and mapping.

In addition to sensors, the selection of classifiers is considered important for the discrimination and detection of invasive plants species [20]. Various classifiers, including maximum likelihood, k-means, nearest-neighbour classification, fuzzy classification, neural networks, support vector machines, random forests, minimum distance, etc., have been used for invasion monitoring in different parts of the world [23]. However, machine learning (ML) algorithms are reported to map the invasive species with higher classification accuracies. Contrary to the statistical approaches, ML methods are non-parametric, since they do not rely on any assumption about the data distribution [24]. Dube et al. [25] used moderate-resolution data from Sentinel-2 (10 m) and Landsat (30 m) to characterize the invasive *L. camara* in the rangeland ecosystems of South Africa and achieved 83% classification accuracy with a random forest classifier. Rajah et al. [26] used a support vector machine algorithm to discriminate *Rubus cuneifolius* Pursh (an invasive plant species in South Africa) with 80% accuracy using a fusion of Sentinel-2 and SAR imagery of Sentinel-1. *Spartina alterniflora* Loisel. (an invasive plant in China) was detected by using a random forest classifier in multitemporal images of Sentinel-2 and Landsat-8 with overall accuracies of 82.8% and 77.8%, respectively [27]. Another invasive species, *Rhamnus frangula* L., was detected with 69% accuracy in forest regions of Québec, Canada, by using linear spectral mixture models on Landsat 8 OLI images [28].

In addition to classification methods and satellite sensors, statistical tools and software-based packages also have great importance in detecting and mapping invasive flora. dzetsaka is one of the classification tools in QGIS (developed in 2016 [29]) that allows the user to classify images with different ML algorithms [30]. This plugin has been successfully used to delineate vegetation in Guiana Amazonian Park in France [31] and for mangrove forest mapping in Cambodia [32]. However, its application in monitoring of invasive species is not reported much yet. Recently, the invasion of *Hedychium coronarium* J. König was mapped in the riparian forests of Brazil using dzetsaka ML algorithms [33].

The application of remote sensing in mapping the distribution of invasive species in natural areas has not been investigated in detail in Pakistan. A few attempts have been made for vegetation cover mapping by researchers from the University of Karachi [34]. *Prosopis juliflora* (Sw.) DC. (a woody invasive species) was mapped in a 16 km^2 area in Karachi, Pakistan, by using high-resolution Worldview-2 imagery and object-based classification [35]. Similarly, *P. juliflora* was also mapped in Karachi using spectral angle mapper classifier in EO-1 hyperspectral imagery with 69% accuracy [36]. Recently, parthenium weed, *Parthenium hysterophorus* L. (an invasive herb), was mapped in some arable lands of Punjab and Khyber Pakhtunkhwa provinces of Pakistan [37].

To the best of our knowledge, no studies on mapping of invasive species using multispectral data in forest ecosystems or protected areas have been conducted in Pakistan thus far, other than ours. It is the need of the hour to start monitoring some of the important

forest invasive species in Pakistan to delimit or better manage these species in order to protect the high-value assets. Therefore, the current study was carried out to map the distribution of native (*D. viscosa*) and invasive species (*L. camara* and *L. leucocephala*) in two reserve forests using the PlanetScope and Sentinel-2 imagery data and to compare different machine learning algorithms for classification of these species.

2. Materials and Methods

2.1. Site Description

The study area covered two scrub forests of Jhelum, a district of the Punjab province, Pakistan (Figure 1). The Lehri Reserve Forest (33.15°N, 73.59°E) covers an area of 4843 hectares, and the Jindi Reserve Forest (33.06°N, 73.47°E) extends over 2163 hectares (Figure 2), consisting of 41 and 16 forest blocks, respectively. Collectively, both forests are called the Lehri Nature Park, classified as a Reserve Forest in 1987 by the state government for the protection and conservation of natural flora and fauna of the park. We use the combined name, Lehri–Jindi Reserve Forest, in the current study. Both forests have semi-evergreen scrub vegetation and are in the east of the salt range. Their elevation ranges from 250 to 1025 m [38]. Topographically, the area is rugged with steep, low mountains covered with dense vegetation.



(**a**) (**b**)

Figure 1. Topography of the study area showing rugged and steep mountains (**b**) and dry scrub vegetation (**a**).

The native vegetation is mainly subtropical dry evergreen open scrub, dominated by *Dodonaea viscosa* (L.) Jacq., *Acacia modesta* Wall., *Olea ferruginea* Wall. ex Aitch., *Ziziphus nummularia* (Burm.f.) Wight and Arn., and *Prosopis juliflora* L.; and grasses such as *Heteropogon contortus* L. [39]. Dominant invasive species of the study area were *Lantana camara* L., *Leucaena leucocephala* L., and *Prosopis juliflora* L. [40].

2.2. Selection of Target Species

One native species (*Dodonea viscosa*) and two invasive species (*Lantana camara* and *Leuacaena leucocephala*) that are dominant in the study area [40] were prioritized for distribution mapping using image classification. Both plants are reported as invasive species in Pakistan. However, they were not previously reported in the study area; therefore, they were selected for distribution mapping.

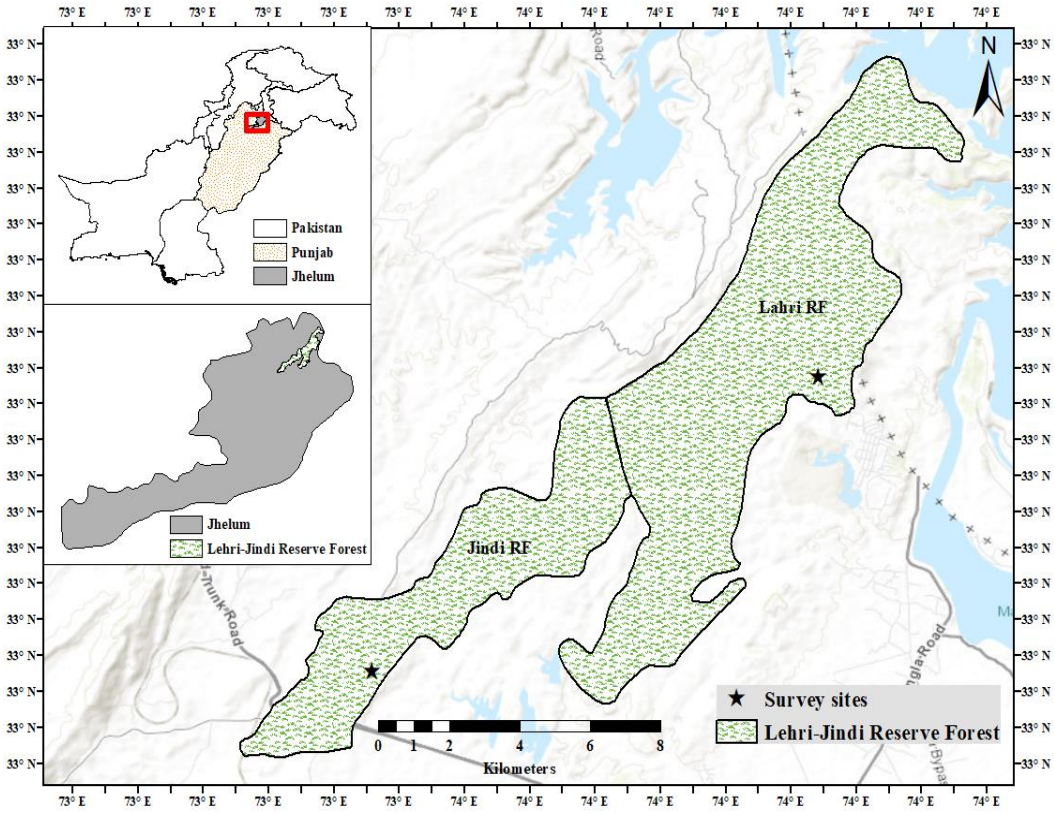


Figure 2. Map of the study area showing survey sites, located in North Jhelum in Punjab, Pakistan.

2.3. Field Data Collection

To map the distribution of invasive species, ground-based locality data of vegetation was required. A few field surveys were undertaken in Lehri–Jindi Reserve Forest during 2018–2020 to collect training data from the accessible sites within the study area (Figure 2). A random sampling technique was used to select the sites where ground truth points of different plant species were recorded. During fieldwork, we tried to capture data for each class, with the minimum presence of two individual plants, having at least 1.5 m ground cover. The geo-referenced data points were collected with the help of a hand-held GPS (model ETREX 20, GARMIN) with an accuracy of ±3 m. At each sampling point, the name of the plant species, its habit, and growth conditions were recorded, along with coordinates. Digital photographs of locations and plants were also taken for reference. A total of 511 training points for 5 different classes (*Lantana camara*, *Leucaena leucocephala*, *Dodonaea viscosa*, other vegetation and non-vegetation) were collected from different locations of the Lehri–Jindi Reserve Forest.

The geographic boundaries of Lehri–Jindi Reserve Forest were digitized after georeferencing a scanned map acquired from the Provincial Forest Department. The map was georeferenced by using the Georeferencing tool in ArcGIS 10.6 with coordinate system UTM zone 43 and datum WGS84. Digitization was performed by using this map and some boundary location points (from Google Earth Pro) to get the final shapefile of the study area.

2.4. Satellite Data Acquisition

Two satellite datasets of different resolution were selected for mapping invasive species in both forests. Sentinel-2 (10 m) and PlanetScope (3 m) images were acquired from online resources, as both have multispectral moderate to high-resolution sensors and are freely available.

2.4.1. Sentinel-2

The Sentinel-2 mission is a constellation of two optical twin satellites. Sentinel-2A (launched in 2015) and Sentinel-2B (launched in 2017) provide global coverage of the Earth's surface with a 290 km field view in a single image [41]. The spectral resolution of Sentinel-2 consists of 13 multispectral bands with a spatial resolution of 10, 20, and 60 m and a temporal resolution of 5 days [42].

For the current study, an image of Sentinel-2B was downloaded from the Copernicus Open Access Hub (https://scihub.copernicus.eu/ (accessed on 5 August 2020)) using forest vector boundaries. Level-2A image was downloaded because it is already processed by ESA using the Sen2Cor algorithm. Therefore, all bands of downloaded imagery were already georeferenced, orthorectified, and radiometrically calibrated [43]. Only the 60 m resolution bands were excluded from this study. Specifications of the selected bands are presented in Table 1. The image obtained was on the same day (8–9 October) and year (2018, 2019) when most of the training samples were taken from the field (Table 2).

Table 1. Band specifications of Sentinel-2B product used in the study.

Bands	Central Wavelength (nm)	Resolution (m)
Band 2—Blue	490	10
Band 3—Green	560	10
Band 4—Red	665	10
Band 5—Vegetation red edge	705	20
Band 6—Vegetation red edge	740	20
Band 7—Vegetation red edge	783	20
Band 8—NIR	842	10
Band 8A—Narrow NIR	865	20
Band 11—SWIR	1610	20
Band 12—SWIR	2190	20

Table 2. An overview of product images of the study area obtained from different satellites.

Tile No	Acquisition Date	Sensor	Cloud Cover	Spatial Resolution
S2B_MSIL2A_20191008T054719 _N0213_R048_T43SCS_20191008T095930	8 October 2019	Sentinel-2	0.08%	10 m
20191009_052515_100c_3B	9 October 2019	PlanetScope	0%	3 m
20191009_052516_100c_3B	9 October 2019	PlanetScope	0%	3 m
20191009_052517_100c_3B	9 October 2019	PlanetScope	0%	3 m
20191009_052518_100c_3B	9 October 2019	PlanetScope	0%	3 m

2.4.2. PlanetScope

PlanetScope is a constellation consisting of more than 130 satellites that are operated by Planet Labs and provide global coverage on a daily basis [44]. PlanetScope (PS) imagery consists of a total of four spectral bands, blue (455–515 nm), green (500–590 nm), red (590–670 nm), and near-infrared NIR (780–860 nm) with a spatial resolution of 3 m [45]. For the current study, four cloud-free PS level 3B images were ordered from Planet Labs (https://www.planet.com/ (accessed on 5 August 2020)) with the dates that coincided with the field visits (Table 2). These level 3B scenes had radiometric and sensor corrections and were already atmospherically corrected in UTM Geographic Long/Lat Projection, Datum WGS84, and zone 43 [46].

2.5. Data Processing

Datasets obtained from satellite imagery (PlanetScope and Sentinel-2 data) and ground truth data were further processed to extract useful information required to map invasive plant species.

2.5.1. Field Data Processing

The training points collected from GPS devices during all visits were exported to an Excel spreadsheet, and temporary codes were replaced with actual plant species names along with their other descriptions (habit, categories, growth stage, etc). To make a layer shapefile for ground-truth data, the Excel file was converted into a point shapefile (.shp format) by using conversion tools in ArcGIS 10.6. A total of 5 classes (*L. camara*, *L. leucocephala*, *D. viscosa*, non-vegetation, and other vegetation) were made with the field data. The buffer tool was used to convert the point shape file (having specific GPS locations of all classes) into a 1m polygon shapefile. Buffering of these training samples helped to extract more spectral information from satellite data. This vector file was further used during classification.

2.5.2. Satellite Data Processing

The two image scenes acquired from Sentinel-2 and PlanetScope were further preprocessed before classification. Sentinel-2 data have spectral bands of different spatial resolutions. Therefore, it was necessary to convert the raster pixel size before processing. All 20 m bands (B5, B6, B7, B11, B12, BA) were resampled to 10 m resolution using the ArcGIS resample method in the data management tools. After that, band stacking was carried out for all 10 bands, including the blue (490 nm), green (560 nm), red (665 nm), and near-infrared (842 nm) bands, using the ArcGIS composite band tool. Finally, the Sentinel-2 imagery was subset according to the study area by using ArcGIS 10.6. Similarly, with PlanetScope data, all four tiles were mosaicked to make one complete scene using ArcGIS 10.6 and further clipped to the study area extent, resulting in required imagery.

2.6. Species Distribution Mapping

This step involved the classification of plant species based on the training data. The pixels having similar reflectance were classified as the same class. For the current study, a supervised classification method was performed by using machine learning algorithms with the dzetsaka classification tool in QGIS [29].

2.6.1. Machine Learning Algorithms

Four non-parametric classifiers, random forest (RF), support vector machine (SVM), Gaussian mixture model (GMM), and k-nearest neighbour (KNN) were used to classify the Sentinel-2 and PlanetScope images. The random forest algorithm is a combination of decision trees that can model a high-degree nonlinear relationship between the targeted and predicted variables [24,47]. It uses bootstrap aggregation to create multiple formations of subsets for obtaining variety of trees [24]. The random forest classifier combines multiple decision tree classifiers applied to a sample from the input data vector. Each decision tree casts a vote for the most likely class [24]. The random forest classifier uses the Gini index to select attributes that predict the classes. For a given training set T, by selecting one case (pixel) at random and saying that it belongs to some class C_i, the Gini index can be written as:

$$\sum \sum_{j \neq i} \left(f(C_i, T)/|T| \right) \left(f\left(C_j, T\right)/|T| \right) \quad (1)$$

where $f(C_i,T)/|T|$ is the probability that the selected pixel belongs to class C_i [48].

The random forest chooses the class for each pixel that receives the most votes. SVM, developed by Cortes and Vapnik, [49], is a linear model for classification and regression problems that is mainly based on kernels. The kernel implemented in dzetsaka is the radial basis function (a Gaussian kernel) which provides high quality results in tree species classification [31]. SVMs have been applied widely in remote sensing [50]. A mathematical formulation of the SVM can be found in Scikit learn [51,52].

GMM is one of the fastest algorithms available in dzetsaka that accounts for the sum of several Gaussian processes [29]. A Gaussian mixture model is a weighted sum of M component Gaussian densities, as given by

$$p(x|\lambda) = \sum_{i=1}^{M} \omega_i g\left(x \middle| \mu_i, \sum_i\right) \quad (2)$$

where x is a D-dimensional continuous-valued data vector, w_i, $i = 1, \ldots, M$, are the mixture weights, and $g(x \mid \mu i, \Sigma i)$, $i = 1, \ldots, M$, are the component Gaussian densities. Each component density is a D-variate Gaussian function of the form

$$g\left(x \middle| \mu_i, \sum_i\right) = \frac{1}{(2\pi)^{D/2}|\sum_i|^{1/2}} \exp\left\{-\frac{1}{2}(x-\mu_i)' \sum_i^{-1}(x-\mu_i)\right\} \quad (3)$$

with mean vector μ_i and covariance matrix Σ_i [53].

The model assumes all data points are obtained from a mixture of finite Gaussian distributions with unknown parameters. Similarly, k-NN is a simple ML algorithm that is used to solve both classification and regression problems [54] and based on the k nearest neighbours, where k is a specified integer value [29]. In the dzetsaka plugin, this parameter (number of neighbours) is chosen in a cross-validation method to maximize the quality of results [31].

2.6.2. Dzetsaka Plugin in QGIS

The dzetsaka classification plugin allows the user to classify images with several machine learning algorithms. It was installed in QGIS from the plugin's menu. However, to use all algorithms in dzetsaka, some dependencies had to be installed. Scikit-learn is the reference Python library for machine learning. All four classifiers were run on both sensor images, and the output raster was generated. Default parameters of dzetsaka plugin were used to run all algorithms. Two invasive (*L. camara* and *L. leucocephala*) and one native species (*D. viscosa*) were targeted for mapping inside forests. Therefore, a total of 5 classes; *L. camara*, *L. leucocephala*, *D. viscosa*, other vegetation and non-vegetation, were trained for classification. A confusion matrix, generated during all classifications, was saved in a separate directory for the measurement of classification accuracy. A ratio of 70:30 was used to partition training: validation data.

2.7. Accuracy Assessment

The results of classifications were evaluated by a confusion matrix, produced by the dzetsaka plugin for all classifiers and sensors. User accuracies (UA), producer accuracies (PA), overall accuracy (OA), and the kappa coefficient (K) were calculated for all assigned classes [55]. The equations for calculation of UA, PA, OA, and kappa were:

$$Producer's\ accuracy = \frac{\text{Number of correctly classified pixels of a class}}{\text{Sum producer in a column}} \quad (4)$$

$$User's\ accuracy = \frac{\text{Number of correctly classified pixels of a class}}{\text{Sum user in a row}} \quad (5)$$

$$Overall\ accuracy = \frac{\text{Sum of correctly classified pixels}}{\text{Sum of pixels used for accuracy assessment (N)}} \quad (6)$$

$$Kappa = \frac{\text{Observed accuracy} - \text{Expexted accuracy}}{1 - \text{Expected accuracy}} \quad (7)$$

2.8. Cover Percentages of Classes

The percentage cover of each class (classified) was calculated using the post-processing tool from the Semi-automatic Classification Plugin (SCP) within QGIS. Pixel counts for

each class were extracted via SCP > Post-processing > Classification report. Later, these pixel counts were used to determine the areas of native and invasive species. The following equation for calculating the area of each class was used:

$$Area = \frac{Pixel\ size\ of\ sensor \times pixel\ count\ of\ each\ class}{10,000} \quad (8)$$

2.9. Distribution Map

After classification, the output rasters from Sentinel-2 and PlanetScope were used to develop the final class distribution maps in Arcmap 10.6. Firstly, the classified raster map of each ML algorithm was converted into vector polygon data using Polygonize tool in QGIS. Then, classified polygon data were exported in Arcmap 10.6, where final distribution maps of all classifiers with both sensors were developed. These maps were compared, along with both algorithms and sensors.

3. Results

3.1. Classification with PlanetScope Satellite (3 m)

A total of four different ML classifiers were tested for the ability to map the distribution cover of invasive species in the Lehri–Jindi Reserve Forest. The bands in the blue, green, red, and near-infrared ranges of the electromagnetic spectrum from the PlanetScope satellites were able to detect all five classes (*L. camara*, *L. leucocephala*, *D. viscosa*, non-vegetation, and other vegetation) using all ML classifiers. The confusion matrices of the classifications are presented in Table S1. The range of overall accuracy of classification with different algorithms was found to be 57–64% (Table 3). Among the different classifiers, random forest (RF) showed the highest classification performance with an overall accuracy of 64% and kappa of 0.53, followed by a Gaussian mixture model (GMM) with an overall accuracy of 63% and kappa of 0.53 (Table 3). The lowest accuracy was found to be 57% (kappa 0.43) with the k-nearest neighbour classifier using 3 m spatial resolution (Table 3).

Table 3. Overall accuracy (%) and kappa coefficient values of four different ML algorithms used to classify PlanetScope satellite imagery.

ML Algorithms	Overall Accuracy (%)	Kappa
Random forest (RF)	64	0.53
Gaussian mixture model (GMM)	63	0.53
K-Nearest neighbor (KNN	57	0.44
Support vector machine (SVM)	58	0.45

Different ML algorithms showed variations in the user and producer accuracies of different classes mapped. In most cases, higher user and producer accuracy were obtained through the RF algorithm for all classes (Figure 3). For *L. camara* (invasive), the user accuracy and producer accuracy were 11–44% and 22–43%, respectively (Figure 3a). Similarly, *L. leucocephala* (invasive) obtained the highest user and producer accuracy of 100% and 88% respectively, with the KNN algorithm (Figure 3b). However, *D. viscosa* (native) was detectable with less accuracy (<45%) for all algorithms, especially with the KNN algorithm (Figure 3c).

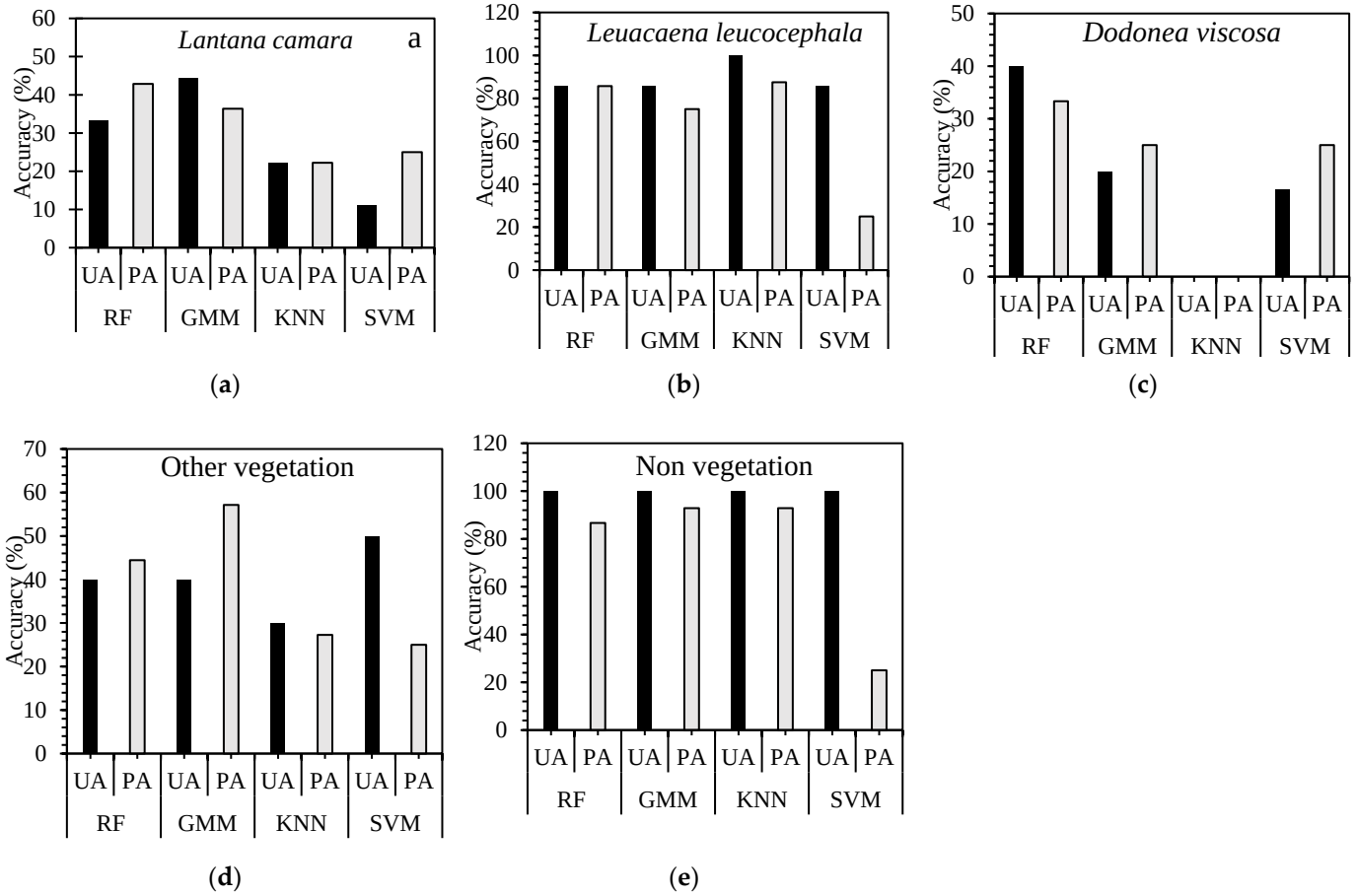


Figure 3. Graphical representation of user accuracy (UA) and producer accuracy (PA) for PlanetScope data with all classes. *Lantana camara*, (**a**) *Leucaena leucocephala*, (**b**) *Dodonaea viscosa*, (**c**) other vegetation, (**d**) and non-vegetation (**e**).

Among the five classes, maximum user and producer accuracies were observed for the non-vegetation class (Figure 3e). For example, non-vegetation showed >80% user and producer accuracies with all algorithms, except the producer accuracy of 25% with the SVM algorithm (Figure 3e). Similarly, *L. leucocephala* also showed >70% user and producer accuracies with all algorithms, except producer accuracy of 25% with the SVM algorithm (Figure 3b).

The classification output maps showed that different ML algorithms were able to discriminate and detect the cover of all classes (Figure 4). The RF algorithm discriminated the vegetation (native, invasive, and other) and non-vegetation classes with the highest accuracy (Figure 4a). The RF algorithm shows that *L. camara* (invasive species) has invaded a total area of 1633 hectares (24%) in the Lehri–Jindi RF (Figure 4a; Table A1). The output map showed that *Lantana* infestation was spread across the reserve forest. Similarly, *L. leucocephala* (invasive) covered an area of 447 hectares that corresponds to 7% of the total study area. Most of the *L. leucocephala* infestation was distributed in the south of Jindi Reserve Forest (Figure 4a). The cover of *D. viscosa* (native) was 7% (494 hectares) of the total study area. Other vegetation also covered 24% (1656 hectares) in the Lehri–Jindi Reserve Forest. Mostly bare areas (non-vegetation) were observed in Jindi Reserve Forest, which covered 2595 hectares (38%).

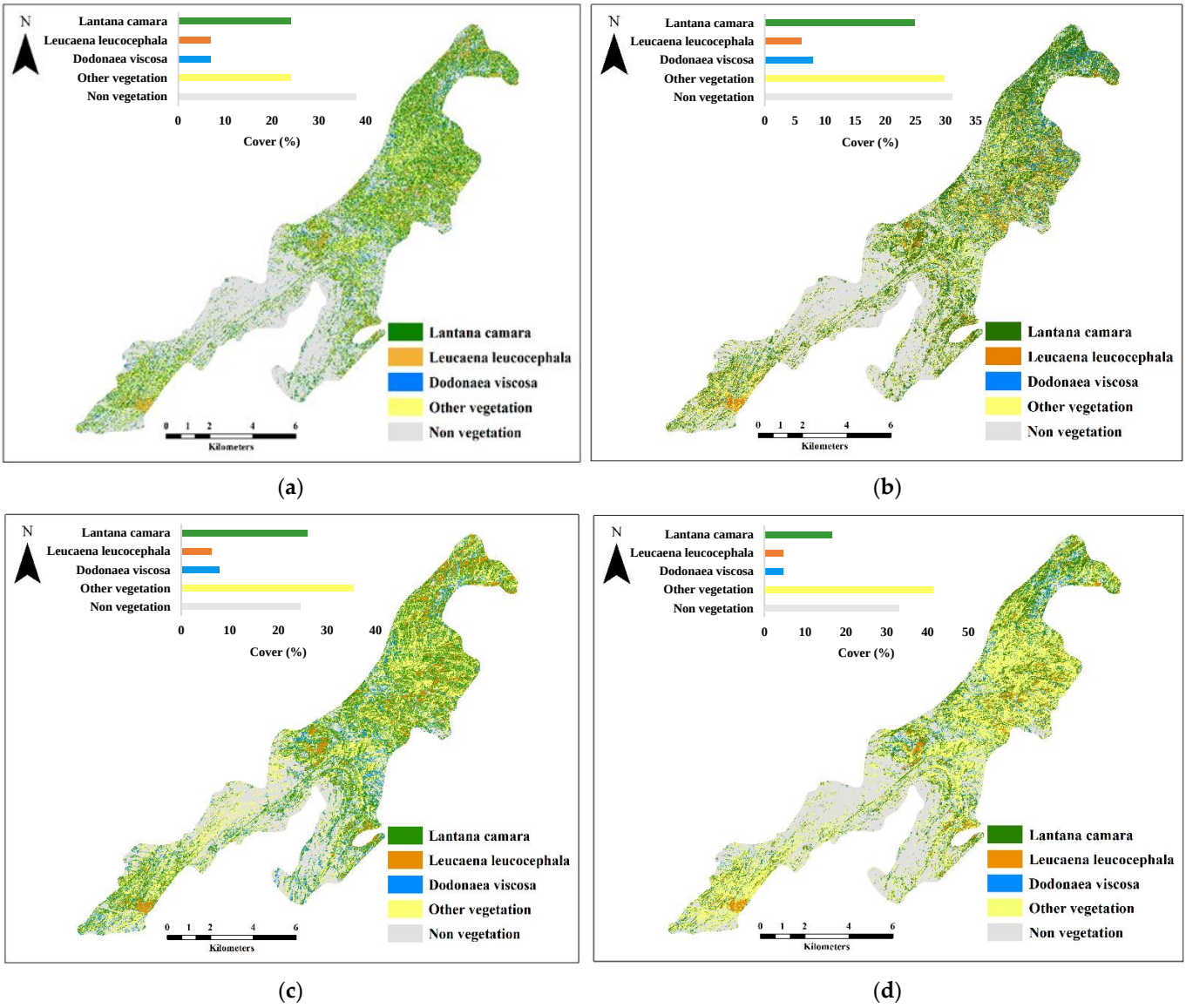


Figure 4. Distribution cover map of five classes in Lehri–Jindi Reserve Forest generated through different classification approaches using PlanetScope data. Random forest, (**a**) Gaussian mixture model, (**b**) k-nearest neighbour, (**c**) support vector machine (**d**).

Distribution maps developed based on other algorithms showed more or less similar results as those of the RF algorithm (Figure 4b–d). For instance, GMM and KNN showed the infestation of *L. camara* (invasive) over an area of 1698 hectares (25%) or 1773 hectares (26%), respectively (Figure 4b,c). Similarly, the cover area invaded by *L. leucocephala* was 6% of total study area using both GMM and KNN classifiers (Table A1).

Lantana camara was the most dominant plant species (23%) represented in all thematic maps (Figure 4). *D. viscosa* (native) was represented mainly in the northern parts of Lehri Reserve Forest, as represented in blue shade in all maps. However, the SVM algorithm showed a different distribution pattern (due to less overall accuracy) of classes than outputs of other algorithms (Figure 4d). For example, a large area of 2816 hectares (41%) was found to be covered by other vegetation, mapped through SVM (Figure 4d). There was a replacement of *L. camara* with the class other vegetation that represents mixing of classes on the map (Figure 4d).

3.2. Classification with Sentinel-2 Satellite (10 m)

Results revealed that the bands in the blue, green, red, red-edge, and NIR domains from the Sentinel-2 satellites were able to detect all five classes using three ML classifiers (except SVM). The confusion metrices of classifications are presented in Table S1. The range of overall accuracy with different algorithms was found to be 55–59% (Table 4). Among different classifiers, the k-nearest neighbour (KNN) algorithm showed the highest classification performance with an overall accuracy of 59% and kappa of 0.47 (Table 4). Similarly, random forest (RF) also mapped all classes with an overall accuracy of 58% and kappa of 0.46. The lowest accuracy was 55% (kappa 0.42), by the support vector machine algorithm (Table 4).

Table 4. Overall accuracy (%) and kappa coefficient values of four different machine learning (ML) algorithms used to classify Sentinel-2 satellite imagery.

ML Algorithms	Overall Accuracy (%)	Kappa
Random forest (RF)	58	0.46
Gaussian mixture model (GMM)	57	0.43
K-Nearest neighbor (KNN)	59	0.47
Support vector machine (SVM)	55	0.42

Different ML algorithms had variations in user and producer accuracies for the different classes. Like the PlanetScope (3 m) classification results, the higher user and producer accuracies were obtained from the RF algorithm for all classes (Figure 5). For *L. camara* (invasive), the user accuracy and producer accuracies were 48–93% and 38–48% respectively (Figure 5a). Similarly, *L. leucocephala* (invasive) obtained the highest user accuracy of 75% with the KNN algorithm (Figure 5b). However, the highest producer accuracy (85%) for *L. leucocephala* was achieved with the GMM algorithm (Figure 5b).

Similar to the PlanetScope findings, maximum user and producer accuracies were achieved in the non-vegetation class among all five classes (Figure 5e). For example, non-vegetation showed >75% user and producer accuracies with all algorithms, except the producer accuracy of 0% with the SVM algorithm (Figure 5e). The SVM algorithm was not able to detect *D. viscosa* or other vegetation using Sentinel data, and hence achieved 0% user and producer accuracies (Figure 5c,e).

The final thematic maps produced from different ML algorithms were able to classify all classes, except the SVM algorithm (Figure 6). The k-nearest neighbour (KNN) algorithm discriminated the vegetation (native, invasive, and other) and non-vegetation classes with the highest accuracy on the thematic map (Figure 6c). Using the KNN algorithm, *L.camara* (invasive) was able to show the total infestation of 2954 hectares, which constituted 43% of total study area cover (Figure 6c; Table A1). Similarly, *L. leucocephala* (invasive) covered an area of 257 hectares, which corresponds to 4% of total study area cover. Similar to PlanetScope classification, much of the *L. leucocephala* infestation was present in the south of Jindi Reserve Forest (Figure 6c). The cover of *D. viscosa* (native) was also 6% (428 hectares) of total study area.

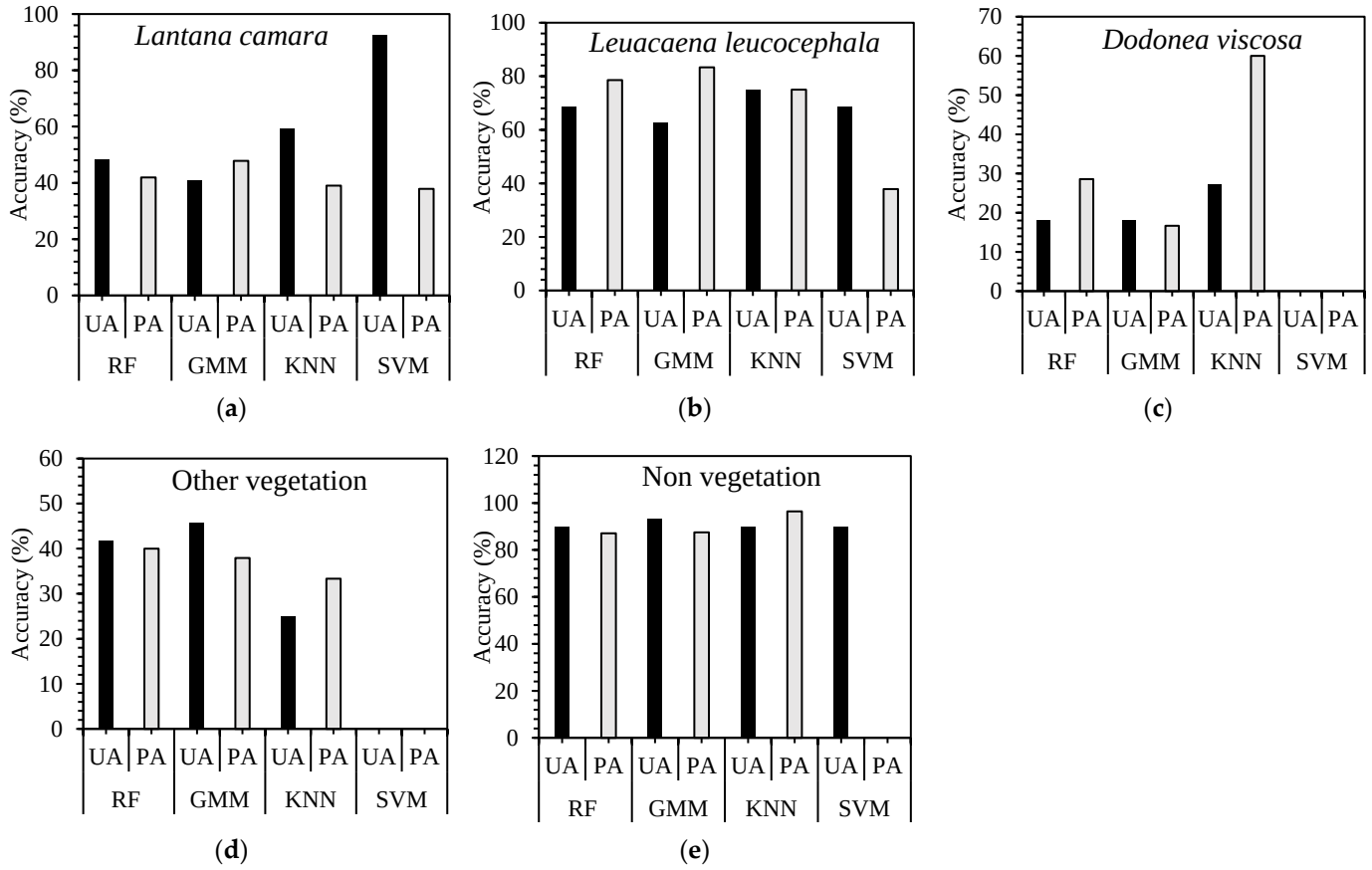


Figure 5. Graphical representation of user accuracy (UA) and producer accuracy (PA) for Sentinel-2 data with all classes. *Lantana camara*, (**a**) *Leucaena leucocephala*, (**b**) *Dodonaea viscosa*, (**c**) other vegetation, (**d**) and non-vegetation (**e**).

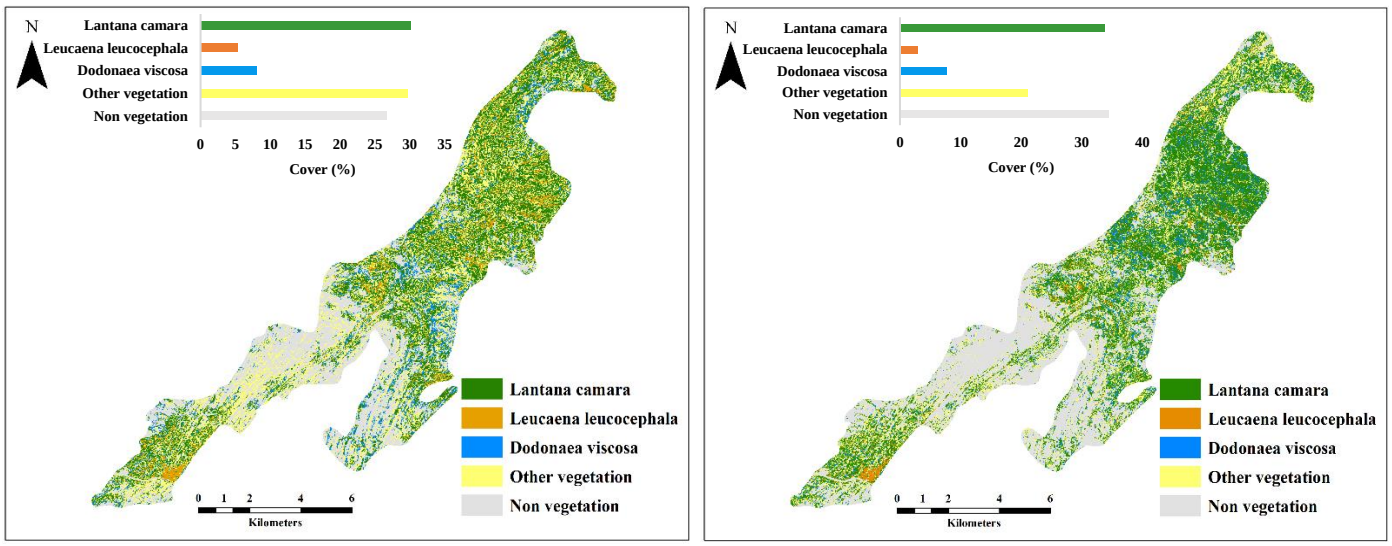


Figure 6. *Cont.*

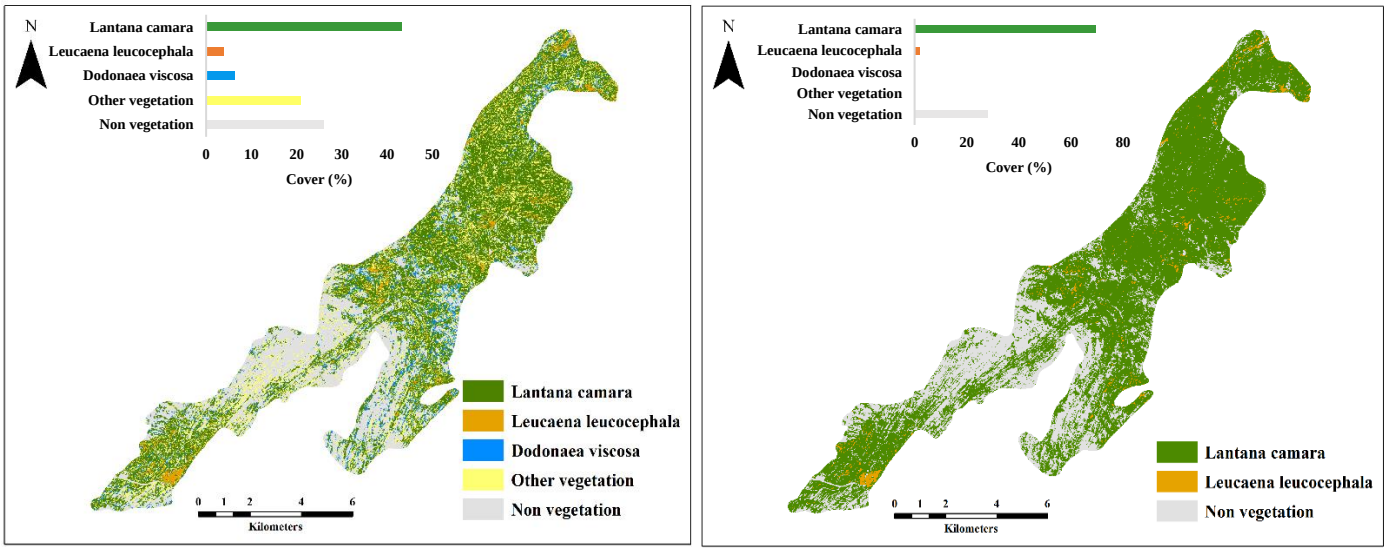


Figure 6. Distribution cover map of five classes in the Lehri–Jindi Reserve Forest generated through different classification approaches using Sentinel data. Random forest, (**a**) Gaussian mixture model, (**b**) k-nearest neighbour, (**c**) support vector machine (**d**).

Distribution maps generated based on other algorithms also showed more or less similar results (like the RF algorithm) using the Sentinel-2 data (Figure 6a,b,d). For example, RF and GMM showed the infestation of *L. camara* (invasive) over areas of 2063 hectares (30%) and 2309 hectares (34%), respectively (Figure 6a,b; Table A1). Similarly, the cover area invaded by *L. leucocephala* was 5% or 3% of total study area using the RF or GMM, respectively (Table A1). *Dodonaea viscosa* was found to cover an area of 550 hectares (8%) and 530 hectares (8%), using the RF and GMM respectively.

L. camara was the most dominant plant species among the individual plant species classes (Figure 6). However, it was not possible to discriminate and map *D. viscosa* and other vegetation classes using the SVM with Sentinel-2 data. Therefore, the SVM algorithm misclassified much of the areas as *L. camara* only, 70% of the total map (Figure 6d).

3.3. Comparison between PlanetScope and Sentinel-2

Results indicated that both satellite types and classification algorithms tended to identify the same general areas on the maps as invasive species, although there were some variations among the maps, and a few exceptions. The average classification results of PlanetScope imagery (3 m resolution) were found to be 5% more accurate than the Sentinel-2 imagery (10 m) with the RF, GMM, and SVM algorithms (Figure 7). Among the classifiers, RF obtained the highest accuracy of 64%. Only the KNN algorithm had higher accuracy using Sentinel-2 data instead of PlanetScope data (Figure 7).

It was observed that Sentinel-2 mapping resulted in a higher percentage cover of *L. camara* with all classifiers than in the PlanetScope mapping (Figure 8a). Conversely, *L. leucocephala* was mapped to have higher coverage using Sentinel-2 imagery than PlanetScope imagery with all classifiers (Figure 8b).

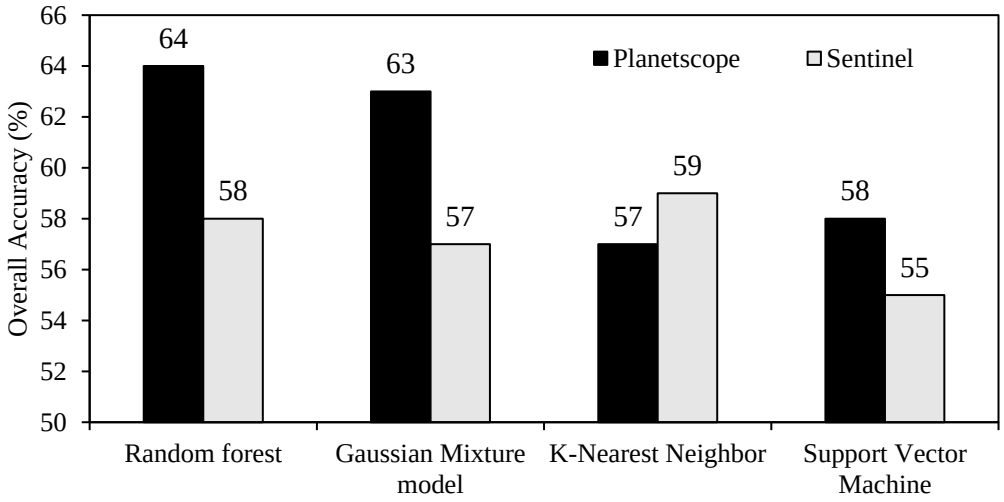


Figure 7. Graphical representation of overall accuracy of all ML algorithms with PlanetScope and Sentinel-2 data.

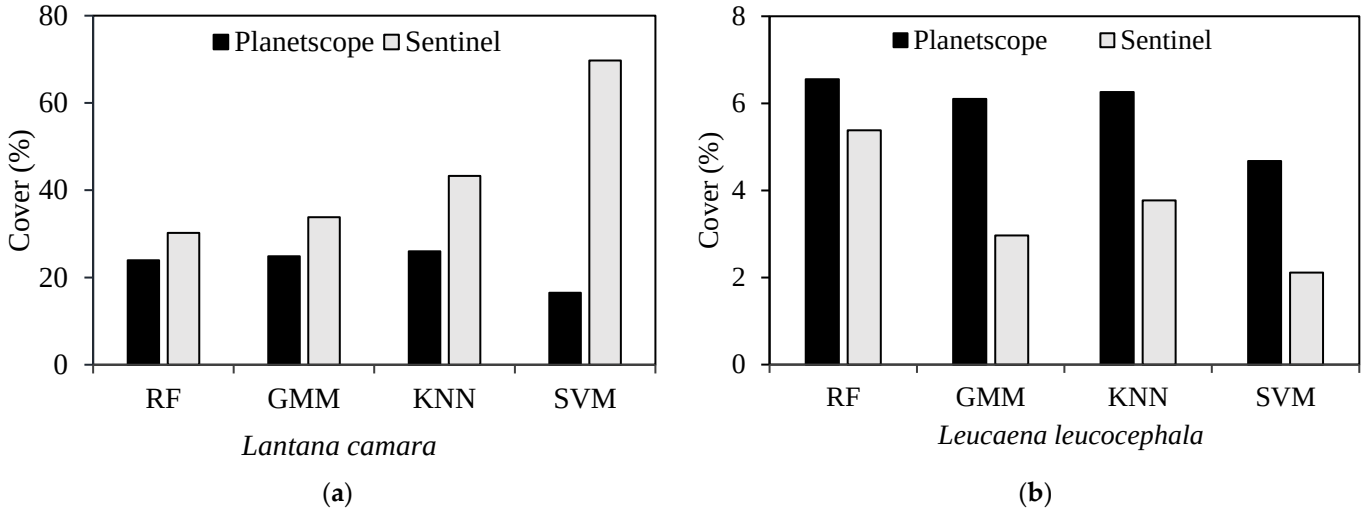


Figure 8. Graphical representation of cover percentage sof *L. camara* (**a**) and *L. leucocephala* (**b**) using all ML algorithms with PlanetScope and Sentinel-2 data.

4. Discussion

The systematic monitoring of invasive alien plant species through remote sensing techniques is essential for the biodiversity conservation and sustainable forest management [12,56]. Multispectral remote sensing of invasive species provides a permanent spatial record that helps to monitor the distribution patterns of invasion in protected areas over time [57].

The overall accuracy (OA) on the PlanetScope and Sentinel-2 datasets was found to be 55–64%; all algorithms were not much different, although differences in the pixel size (spatial resolution) exist between the sensors (Tables 2 and 3). The reason may have been the high spectral resolution of Sentinel-2 datasets, which contain 13 different spectral bands, including NIR and unique red-edge bands, which provide more support in the spectral separability of different species [27,58]. The red-edge region is especially interesting, as Sentinel-2 offers more bands in this spectral range than comparable satellite missions, and it has more power to characterise the variations in vegetation condition [42]. These bands are absent in PlanetScope datasets. Conversely, it was observed that the producer accuracy (PA) of all land cover classes was higher with PlanetScope than with Sentinel-2. This was likely due to the high spatial resolution (3 m) of PlanetScope, which reduces the prevalence of mixed pixels [59] and accurately detects more variations in smaller pixel size to provide

good results than moderate resolution of Sentinel-2 [60]. Hence, spectral resolution and spatial resolution are equally important in discrimination and accurate mapping of invasive species.

Among different machine learning algorithms, it was observed that the classification results of PlanetScope imagery (3 m) were found to be more accurate than those of the Sentinel-2 imagery (10 m) using RF, GMM, and SVM algorithms (Figure 7). The RF algorithm yielded the best results with the highest accuracy (64%) using PlanetScope data (Table 2). These findings are similar to several other studies on alien species mapping, where the RF algorithm resulted in highest accuracy [61,62]. Due to the non-parametric nature and high classification accuracy, RF classification has several advantages over other classifiers [63,64]. Although it produces complex decision trees, it reduces the operational and computational costs using training samples without sacrificing too much accuracy [65].

The results of the current study were based on freely available satellite data, open-source machine learning algorithms, and free software (QGIS). This means that the use of open-source classifiers and multispectral sensors is effective at producing distribution maps of invasive species and other vegetation [33,59,66]. Moreover, the dzetsaka plugin of QGIS is able to classify the vegetation types from multispectral images [31,67]. This plugin has gained popularity in last 5 years after its development by Karasiak (2016) and is now being used by many scientists for identifying plant species and vegetation cover using different satellite datasets [68,69].

Among the classes mapped in this study, the non-vegetation class was identified with the highest user and producer accuracies (Figure 3e). This may have been due to the distinct spectral signatures of non-vegetation classes (build up, water, bare area) that helped classifiers to discriminate it more accurately. It also depends upon the complexity of land cover classes. Vegetation classes, especially individual plant species, can have similar spectral responses due to their high reflectance peaks in NIR. Therefore, classification of plant species with highest accuracy is still challenging with multispectral sensors [70].

Dodonaea viscosa is a native shrub, but it was detectable with less accuracy (<45%) through all algorithms, especially with the SVM algorithm where discrimination was not possible using the Sentinel-2 dataset (Figure 5c; Figure 6d). Such classification errors are also related species with similar spectral signatures, due to which, mixing of plant species may occur and result in lower accuracies [71]. *Lantana camara* and *D. viscosa* were not well distinguished (with only a few NIR wavebands), even with a hyperspectral sensor [17]. Therefore, it seems justifiable with the current results of multispectral sensors to say that phenological and biophysical responses of both plant species might have been similar at the time of data acquisition.

The overall results of current study represent that PlanetScope and Sentinel-2 datasets have the ability to map the distribution cover of invasive and native plant species in protected areas. Other studies also showed the high performance of both sensors for mapping weeds using ML algorithms [55]. However, the classification results of our study were not as high as other findings reported in the literature. Different factors are involved in getting such results. Firstly, this was due to the spatial and spectral resolution limitations of both sensors (PS and S2) which restrict the accurate discrimination between individual plant species. Secondly, the distribution of different plant species is mapped using these multispectral sensors for different ecosystems and in multiple seasons [27,41,72]. Therefore, the complexity and level of heterogeneity of the scrub forests can also influence the performance of classification. Similarly, phenology (flowering and fruiting phases) at different times of the year also varies and influences the spectral signatures of some plant species [61]. Our results were based on one season only—at the end of summer—however, the study of phenological variations can provide better insights for distribution mapping [13]. For best classification analyses, it would be interesting to perform seasonal studies in the same area, for getting better distinction between native and invasive species. Forest canopy and cloud cover can also influence the results' accuracy, as it gets difficult to detect the small shrub that is under tree canopy or cloud. Moreover, the size of the training

samples also contributes to high accuracy [73]. Our current findings represent the training data of 511 points for accessing the spread and distribution of *L. camara* and *L. leucocephala* due to less accessibility inside forest regions. However, it would be useful to get more training data from the locations to increase the overall accuracy of classification.

Overall, the findings of the current study provide baseline information about the spread of *L. camara* and *L. leucocephala* in the Lehri–Jindi Reserve Forest. It is really alarming to see the high infestation of *L. camara* in almost all blocks of forests. This spread on such a large scale is an emerging threat for the native biodiversity of protected areas. Therefore, early detection of invasive alien plants in Lehri-Jindi RF can provide an efficient mechanism for eradication and for helping the managers to devise adaptive weed management strategies to stop their spread.

5. Conclusions

Remote sensing plays an important role in determining the cover of invasive species in protected areas. The current study aimed to map the cover of *Lantana camara* and *Leucaena leucocephala* in the Lehri–Jindi Reserve Forest using PlanetScope and Sentinel-2 satellite datasets. The accuracy percentages of all ML algorithms were 55–64% using the dzetsaka tool. The highest classification accuracy (64%) was achieved using a random forest algorithm with PlanetScope (3 m resolution). Thus, higher spatial resolution (3 m) helped to discriminate invasive species much better than the low spatial resolution (10 m). The spread of *L. camara* was three times higher than that of *L. leucocephala* in the forests, using the RF algorithm. It was not possible to discriminate *Dodonea viscosa* using sentinel data with the SVM algorithm. Our findings help to better understand and assess the spread of invasive species in topographically challenging and remote regions of the Lehri–Jindi Reserve Forest. The effectiveness of ML algorithms also indicates the usefulness of the dzetsaka plugin in invasion studies. This approach is cost-effective, easy to use, and repeatable way to map the cover of invasive alien plants and help land managers to adopt site-specific mitigation approaches in these invaded areas. It is recommended to evaluate hyperspectral RS data for mapping the invasion using the dzetsaka tool of QGIS in the near future.

Supplementary Materials: The following are available online at https://www.mdpi.com/article/10.3390/rs15041020/s1, Table S1. Confusion matrix of classification using machine learning algorithms (Dzetsaka tool) with Planetscope and Sentinel data.

Author Contributions: Conceptualization, H.B., A.S. and I.M.I.; methodology, H.B. and I.M.I.; software, I.M.I.; writing—original draft preparation, I.M.I.; writing—review and editing, A.S., H.B. and F.-e.-B.; visualization, H.B. and I.M.I.; field survey support, A.S. and F.-e.-B.; supervision, A.S., H.B. and F.-e.-B.; project administration, H.B.; funding acquisition, H.B. and A.S. All authors have read and agreed to the published version of the manuscript.

Funding: This research work was funded by the Higher Education Commission (HEC) of Pakistan through the International Research Support Initiative Program (IRSIP 44/BMS 87). Field based work was funded by Worldwide Fund Pakistan (project no: 50051701). H.B. was supported by the National Centre for Earth Observation, funded by the Natural Environment Research Council, UK (NERC-NCEO). The APC was funded by the Open Access Fund at the University of Leicester with funds from the Natural Environment Research Council, UK.

Data Availability Statement: The data presented in this study are available on request from the corresponding author.

Acknowledgments: We are extremely grateful to the HEC Pakistan for providing funding to do research work with Leicester University. We are also thankful to Muhammad Usman, Sadi Ahmed, and Mubarak Ali for accompanying us during field visits.

Conflicts of Interest: The authors declare no conflict of interest.

Appendix A

Table A1. Area (ha) and percentage cover (%) of different classes using PlanetScope (3 m) and Sentinel-2 satellite datasets.

PlanetScope (3 m)								
Plant species	**RF**		**GMM**		**KNN**		**SVM**	
	Area (ha)	Cover (%)	Area (ha)	Cover (%)	Area (ha)	Cover (%)	Area (ha)	Cover (%)
Lantana camara	1633	24	1698	25	1773	26	1127	17
Leuacaena leucocephala	447	7	417	6	427	6	319	5
Dodonaea viscosa	494	7	549	8	533	8	313	5
Other vegetation	1656	24	2031	30	2420	35	2816	41
Non-vegetation	2595	38	2130	31	1672	24	2250	33
Sentinel (10 m)								
Plant species	**RF**		**GMM**		**KNN**		**SVM**	
	Area (ha)	Cover (%)	Area (ha)	Cover (%)	Area (ha)	Cover (%)	Area (ha)	Cover (%)
Lantana camara	2063	30	2310	34	2954	43	4760	70
Leuacaena leucocephala	367	5	203	3	258	4	144	2
Dodonaea viscosa	550	8	530	8	428	6	0	0
Other vegetation	2026	30	1441	21	1418	21	0	0
Non-vegetation	1820	27	2345	34	1770	26	1924	28

References

1. Blackburn, T.M.; Essl, F.; Evans, T.; Hulme, P.E.; Jeschke, J.M.; Kühn, I.; Kumschick, S.; Marková, Z.; Mrugała, A.; Nentwig, W.; et al. A Unified Classification of Alien Species Based on the Magnitude of Their Environmental Impacts. *PLoS Biol.* **2014**, *12*, e1001850. [CrossRef] [PubMed]
2. Pardo-Primoy, D.; Fagúndez, J. Assessment of the Distribution and Recent Spread of the Invasive Grass Cortaderia Selloana in Industrial Sites in Galicia, NW Spain. *Flora* **2019**, *259*, 151465. [CrossRef]
3. Vilà, M.; Espinar, J.L.; Hejda, M.; Hulme, P.E.; Jarošík, V.; Maron, J.L.; Pergl, J.; Schaffner, U.; Sun, Y.; Pyšek, P. Ecological Impacts of Invasive Alien Plants: A Meta-Analysis of Their Effects on Species, Communities and Ecosystems. *Ecol. Lett.* **2011**, *14*, 702–708. [CrossRef]
4. Matongera, T.N.; Mutanga, O.; Dube, T.; Sibanda, M. Detection and Mapping the Spatial Distribution of Bracken Fern Weeds Using the Landsat 8 OLI New Generation Sensor. *Int. J. Appl. Earth Obs. Geoinf.* **2017**, *57*, 93–103. [CrossRef]
5. Carlier, J.; Davis, E.; Ruas, S.; Byrne, D.; Caffrey, J.M.; Coughlan, N.E.; Dick, J.T.; Lucy, F.E. Using open-source software and digital imagery to efficiently and objectively quantify cover density of an invasive alien plant species. *J. Environ. Manag.* **2020**, *266*, 110519. [CrossRef]
6. Dick, J.T.A.; Alexander, M.E.; Ricciardi, A.; Laverty, C.; Downey, P.O.; Xu, M.; Jeschke, J.M.; Saul, W.C.; Hill, M.P.; Wasserman, R.; et al. Functional Responses Can Unify Invasion Ecology. *Biol. Invasions* **2017**, *19*, 1667–1672. [CrossRef]
7. Caffrey, J.M.; Baars, J.R.; Barbour, J.H.; Boets, P.; Boon, P.; Davenport, K.; Dick, J.T.A.; Early, J.; Edsman, L.; Gallagher, C.; et al. Tackling Invasive Alien Species in Europe: The Top 20 Issues. *Manag. Biol. Invasions* **2014**, *5*, 1–20. [CrossRef]
8. Wang, R.; Gamon, J.A. Remote Sensing of Terrestrial Plant Biodiversity. *Remote Sens. Environ.* **2019**, *231*, 111218. [CrossRef]
9. Juanes, F. Visual and Acoustic Sensors for Early Detection of Biological Invasions: Current Uses and Future Potential. *J. Nat. Conserv.* **2018**, *42*, 7–11. [CrossRef]
10. Müllerová, J.; Brůna, J.; Bartaloš, T.; Dvořák, P.; Vítková, M.; Pyšek, P. Timing Is Important: Unmanned Aircraft vs. Satellite Imagery in Plant Invasion Monitoring. *Front. Plant Sci.* **2017**, *8*, 887. [CrossRef]

11. Bazzichetto, M.; Malavasi, M.; Bartak, V.; Acosta, A.T.R.; Rocchini, D.; Carranza, M.L. Plant Invasion Risk: A Quest for Invasive Species Distribution Modelling in Managing Protected Areas. *Ecol. Indic.* **2018**, *95*, 311–319. [CrossRef]
12. Martinez, B.; Reaser, J.K.; Dehgan, A.; Zamft, B.; Baisch, D.; McCormick, C.; Giordano, A.J.; Aicher, R.; Selbe, S. Technology Innovation: Advancing Capacities for the Early Detection of and Rapid Response to Invasive Species. *Biol. Invasions* **2019**, *22*, 75–100. [CrossRef]
13. Huang, C.; Asner, G.P. Applications of Remote Sensing to Alien Invasive Plant Studies. *Sensors* **2009**, *9*, 4869–4889. [CrossRef] [PubMed]
14. Ismail, R.; Mutanga, O.; Peerbhay, K. The Identification and Remote Detection of Alien Invasive Plants in Commercial Forests: An Overview. *S. Afr. J. Geomat.* **2016**, *5*, 49–67. [CrossRef]
15. Xie, Y.; Sha, Z.; Yu, M. Remote Sensing Imagery in Vegetation Mapping: A Review. *J. Plant Ecol.* **2008**, *1*, 9–23. [CrossRef]
16. Oumar, Z. Assessing the Utility of the Spot 6 Sensor in Detecting and Mapping *Lantana camara* for a Community Clearing Project in KwaZulu-Natal, South Africa. *S. Afr. J. Geomat.* **2016**, *5*, 214–226. [CrossRef]
17. Iqbal, I.M.; Balzter, H.; Firdaus-e-Bareen; Shabbir, A. Identifying the Spectral Signatures of Invasive and Native Plant Species in Two Protected Areas of Pakistan through Field Spectroscopy. *Remote Sens.* **2021**, *13*, 4009. [CrossRef]
18. Transon, J.; d'Andrimont, R.; Maugnard, A.; Defourny, P. Survey of Hyperspectral Earth Observation Applications from Space in the Sentinel-2 Context. *Remote Sens.* **2018**, *10*, 157. [CrossRef]
19. Martin, F.M.; Müllerová, J.; Borgniet, L.; Dommanget, F.; Breton, V.; Evette, A. Using Single- and Multi-Date UAV and Satellite Imagery to Accurately Monitor Invasive Knotweed Species. *Remote Sens.* **2018**, *10*, 1662. [CrossRef]
20. Kopeć, D.; Sabat-Tomala, A.; Michalska-Hejduk, D.; Jarocińska, A.; Niedzielko, J. Application of Airborne Hyperspectral Data for Mapping of Invasive Alien *Spiraea tomentosa* L.: A Serious Threat to Peat Bog Plant Communities. *Wetl. Ecol. Manag.* **2020**, *28*, 357–373. [CrossRef]
21. Skowronek, S.; Ewald, M.; Isermann, M.; van de Kerchove, R.; Lenoir, J.; Aerts, R.; Warrie, J.; Hattab, T.; Honnay, O.; Schmidtlein, S.; et al. Mapping an Invasive Bryophyte Species Using Hyperspectral Remote Sensing Data. *Biol. Invasions* **2017**, *19*, 239–254. [CrossRef]
22. Chen, Y.; Guerschman, J.P.; Cheng, Z.; Guo, L. Remote Sensing for Vegetation Monitoring in Carbon Capture Storage Regions: A Review. *Appl. Energy* **2019**, *240*, 312–326. [CrossRef]
23. Al-Doski, J.; Mansorl, S.B.; Shafri, H.Z.M. *Image Classification in Remote Sensing*; University Putra: Serdang, Malaysia, 2013.
24. Breiman, L. Random Forests. *Mach. Learn.* **2001**, *45*, 5–32. [CrossRef]
25. Dube, T.; Shoko, C.; Sibanda, M.; Madileng, P.; Maluleke, X.G.; Mokwatedi, V.R.; Tibane, L.; Tshebesebe, T. Remote Sensing of Invasive *Lantana camara* (*Verbenaceae*) in Semiarid Savanna Rangeland Ecosystems of South Africa. *Rangel. Ecol. Manag.* **2020**, *73*, 411–419. [CrossRef]
26. Rajah, P.; Odindi, J.; Mutanga, O.; Kiala, Z. The Utility of Sentinel-2 Vegetation Indices (VIs) and Sentinel-1 Synthetic Aperture Radar (SAR) for Invasive Alien Species Detection and Mapping. *Nat. Conserv.* **2019**, *35*, 41–61. [CrossRef]
27. Gong, Z.; Zhang, C.; Zhang, L.; Bai, J.; Zhou, D. Assessing Spatiotemporal Characteristics of Native and Invasive Species with Multi-Temporal Remote Sensing Images in the Yellow River Delta, China. *Land Degrad. Dev.* **2021**, *32*, 1338–1352. [CrossRef]
28. Labonté, J.; Drolet, G.; Sylvain, J.D.; Thiffault, N.; Hébert, F.; Girard, F. Phenology-Based Mapping of an Alien Invasive Species Using Time Series of Multispectral Satellite Data: A Case-Study with Glossy Buckthorn in Québec, Canada. *Remote Sens.* **2020**, *12*, 922. [CrossRef]
29. Karasiak, N. Dzetsaka: Classification Plugin for Qgis. Available online: https://github.com/nkarasiak/dzetsaka (accessed on 3 August 2022).
30. Potić, I.; Potić, M. Remote sensing machine learning algorithms in environmental stress detection—Case study of pan-european south section of corridor 10 in serbia. *Bull. Nat. Sci. Res.* **2017**, *7*, 41–46. [CrossRef]
31. Karasiak, N.; Perbet, P. Remote Sensing of Distinctive Vegetation in Guiana Amazonian Park. *QGIS Appl. Agric. For.* **2018**, *2*, 215–245. [CrossRef]
32. Phorn, N.; Lu, J.; Petchprayoon, P. Mangrove Forests Changes and Responses to Sea Level Rise Based on Remote Sensing and GIS in PKWS, Cambodia. *Intercont. Geoinf. Days* **2021**, *2*, 147–150.
33. Arantes, J.G. Avaliação da Invasão de Hedychium Coronarium J. König (Zingiberaceae) em Florestas Ripárias Usando Algoritmos de Aprendizagem de Máquina e Imagens de Veículo Aéreo Não Tripulado (VANT). Ph.D. Thesis, Universidade Federal de São Carlos, São Carlos, Brazil, 2020.
34. Bano, S.; Afsar, S. Monitoring the plant species through geo-informatics: A case study of karachi university campus, karachi. *Int. J. Biol. Biotech.* **2014**, *11*, 273–285.
35. Shahzad, A.; Jamil Hasan Kazmi, S.; Shahid Shaukat, S.; bin Farhan, S. Survey of Hyperspectral Earth Observation Applications from Space in the Sentinel-2 Context. *Int. J. Biol. Biotech.* **2017**, *14*, 479–484.
36. Kazmi, J.H.; Haase, D.; Shahzad, A.; Shaikh, S.; Zaidi, S.M.; Qureshi, S. Mapping Spatial Distribution of Invasive Alien Species through Satellite Remote Sensing in Karachi, Pakistan: An Urban Ecological Perspective. *Int. J. Environ. Sci. Technol.* **2022**, *19*, 3637–3654. [CrossRef]
37. Huchinson, D. When Astronomers Meet Ecologists: How Remote Sensing Can Tackle Parthenium in Pakistan. Available online: https://blog.invasive-species.org/2018/10/12/when-astronomers-meet-ecologists-how-remote-sensing-can-tackle-parthenium-in-pakistan/ (accessed on 10 January 2022).

38. Saad, M.; Anwar, M.; Waseem, M.; Salim, M. Distribution Range and Population Status of Indian Grey Wolf (*Canis lupus* Pallipes) and Asiatic Jackal (*Canis aureus*) in Lehri Nature Park, District Jhelum, Pakistan. *Pak. J. Anim. Plant Sci.* **2015**, *25*, 433–440.
39. Nawaz, T.; Hameed, M.; Ahmad, F.; Sajid Aqeel Ahmad, M.; Hussain, M.; Ahmad, I.; Younis, A. Khawaja Shafique Ahmad Diversity and Conservation Status of Economically Important Flora of the Salt Range, Pakistan. *Pak. J. Bot.* **2012**, *44*, 203–211.
40. Iqbal, I.M.; Bareen, F.; Shabbir, A. Plant Invasions and Their Impacts on Some Protected Areas of Pakistan. In Proceedings of the Research and Development Congress on Invasive Alien Species (IAS) in the Asia-Pacific, Manila, Phillipines, 8 July 2019; pp. 10–12.
41. Ng, W.T.; Rima, P.; Einzmann, K.; Immitzer, M.; Atzberger, C.; Eckert, S. Assessing the Potential of Sentinel-2 and Pléiades Data for the Detection of Prosopis and Vachellia Spp. in Kenya. *Remote Sens.* **2017**, *9*, 74. [CrossRef]
42. Wessel, M.; Brandmeier, M.; Tiede, D. Evaluation of Different Machine Learning Algorithms for Scalable Classification of Tree Types and Tree Species Based on Sentinel-2 Data. *Remote Sens.* **2018**, *10*, 1419. [CrossRef]
43. Obregón, M.Á.; Rodrigues, G.; Costa, M.J.; Potes, M.; Silva, A.M. Validation of ESA Sentinel-2 L2A Aerosol Optical Thickness and Columnar Water Vapour during 2017–2018. *Remote Sens.* **2019**, *11*, 1649. [CrossRef]
44. Marta, S. Planet Planet Imagery Product Specification. Available online: https://assets.planet.com/docs/Combined-Imagery-Product-Spec-Dec-2018.pdf. (accessed on 11 February 2023).
45. dos Reis, A.A.; Silva, B.C.; Werner, J.P.S.; Silva, Y.F.; Rocha, J.v.; Figueiredo, G.K.D.A.; Antunes, J.F.G.; Esquerdo, J.C.D.M.; Coutinho, A.C.; Lamparelli, R.A.C.; et al. Exploring the potential of high-resolution planetscope imagery for pasture biomass estimation in an integrated crop-livestock system. In Proceedings of the 2020 IEEE Latin American GRSS & ISPRS Remote Sensing Conference (LAGIRS), Santiago, Chile, 22–26 March 2020. [CrossRef]
46. Hang, N.T.T.; Thai Hoa, N.; Phuoc, T.; Son, H.; Nguyen-Ngoc, L. Vegetation Biomass of Sargassum Meadows in An Chan Coastal Waters, Phu Yen Province, Vietnam Derived from PlanetScope Image. *J. Environ. Sci. Eng. B* **2019**, *8*, 81–92. [CrossRef]
47. Ghosh, A.; Sharma, R.; Joshi, P.K. Random Forest Classification of Urban Landscape Using Landsat Archive and Ancillary Data: Combining Seasonal Maps with Decision Level Fusion. *Appl. Geogr.* **2014**, *48*, 31–41. [CrossRef]
48. Pal, M. Random Forest Classifier for Remote Sensing Classification. *Int. J. Remote Sens.* **2007**, *26*, 217–222. [CrossRef]
49. Cortes, C.; Vapnik, V. Support-Vector Networks. *Mach. Learn.* **1995**, *20*, 273–297. [CrossRef]
50. Mountrakis, G.; Im, J.; Ogole, C. Support Vector Machines in Remote Sensing: A Review. *ISPRS J. Photogramm. Remote Sens.* **2011**, *66*, 247–259. [CrossRef]
51. Pedregosa Fabianpedregosa, F.; Michel, V.; Grisel Oliviergrisel, O.; Blondel, M.; Prettenhofer, P.; Weiss, R.; Vanderplas, J.; Cournapeau, D.; Pedregosa, F.; Varoquaux, G.; et al. Scikit-Learn: Machine Learning in Python. *J. Mach. Learn. Res.* **2011**, *12*, 2825–2830.
52. Support Vector Machines—Scikit-Learn 1.2.0 Documentation. Available online: https://scikit-learn.org/stable/modules/svm.html#svm-mathematical-formulation (accessed on 17 January 2023).
53. Reynolds, D. Gaussian Mixture Models. *Encycl. Biom.* **2009**, *741*, 659–663.
54. Jordan, M.I.; Mitchell, T.M. Machine Learning: Trends, Perspectives, and Prospects. *Science* **2015**, *349*, 255–260. [CrossRef]
55. Mudereri, B.T.; Dube, T.; Adel-Rahman, E.M.; Niassy, S.; Kimathi, E.; Khan, Z.; Landmann, T. A Comparative Analysis of PlanetScope and Sentinel-2 Space-Borne Sensors in Mapping Striga Weed Using Guided Regularised Random Forest Classification. *Int. Arch. Photogramm. Remote Sens. Spat. Inf. Sci.* **2019**, *42*, 701–708. [CrossRef]
56. Royimani, L.; Mutanga, O.; Odindi, J.; Dube, T.; Matongera, T.N. Advancements in Satellite Remote Sensing for Mapping and Monitoring of Alien Invasive Plant Species (AIPs). *Phys. Chem. Earth Parts A/B/C* **2019**, *112*, 237–245. [CrossRef]
57. Gil, A.; Yu, Q.; Abadi, M.; Árvore, H.C. Using ASTER Multispectral Imagery for Mapping Woody Invasive Species in Pico Da Vara Natural Reserve (Azores Islands, Portugal). *SciELO Brasil.* **2014**, *38*, 391–401. [CrossRef]
58. Müllerová, J.; Pergl, J.; Pyšek, P. Remote Sensing as a Tool for Monitoring Plant Invasions: Testing the Effects of Data Resolution and Image Classification Approach on the Detection of a Model Plant Species Heracleum Mantegazzianum (Giant Hogweed). *Int. J. Appl. Earth Obs. Geoinf.* **2013**, *25*, 55–65. [CrossRef]
59. Cash, J.S.; Anderson, C.J.; Marzen, L. Evaluating Free and Simple Remote Sensing Methods for Mapping Chinese Privet (*Ligustrum sinense*) Invasions in Hardwood Forests. *SN Appl. Sci.* **2020**, *2*, 789. [CrossRef]
60. Cornejo-Denman, L.; Romo-Leon, J.R.; Hartfield, K.; van Leeuwen, W.J.D.; Ponce-Campos, G.E.; Castellanos-Villegas, A. Landscape Dynamics in an Iconic Watershed of Northwestern Mexico: Vegetation Condition Insights Using Landsat and PlanetScope Data. *Remote Sens.* **2020**, *12*, 2519. [CrossRef]
61. Sabat-Tomala, A.; Raczko, E.; Zagajewski, B. Comparison of Support Vector Machine and Random Forest Algorithms for Invasive and Expansive Species Classification Using Airborne Hyperspectral Data. *Remote Sens.* **2020**, *12*, 516. [CrossRef]
62. Baron, J.; Hill, D.J.; Elmiligi, H. Combining Image Processing and Machine Learning to Identify Invasive Plants in High-Resolution Images. *Int. J. Remote Sens.* **2018**, *39*, 5099–5118. [CrossRef]
63. Sejati, A.W.; Buchori, I.; Kurniawati, S.; Brana, Y.C.; Fariha, T.I. Quantifying the Impact of Industrialization on Blue Carbon Storage in the Coastal Area of Metropolitan Semarang, Indonesia. *Appl. Geogr.* **2020**, *124*, 102319. [CrossRef]
64. Akar, Ö.; Güngör, O. Determination and Analysis of The Agricultural Crops in East Blacksea Region Using Remote Sensing Techonologies. *J. Geod. Geoinf.* **2012**, *1*, 105–112. [CrossRef]
65. Corcoran, J.; Knight, J.; Sensing, A.G.-R. Influence of multi-source and multi-temporal remotely sensed and ancillary data on the accuracy of random forest classification of wetlands in Northern Minnesota. *Remote Sens.* **2013**, *5*, 3212–3238. [CrossRef]

66. Ndlovu, H.S.; Sibanda, M.; Odindi, J.; Buthelezi, S.; Mutanga, O. Detecting and Mapping the Spatial Distribution of Chromoleana Odorata Invasions in Communal Areas of South Africa Using Sentinel-2 Multispectral Remotely Sensed Data. *Phys. Chem. Earth Parts A/B/C* **2022**, *126*, 103081. [CrossRef]
67. Mattivi, P.; Pappalardo, S.E.; Nikolić, N.; Mandolesi, L.; Persichetti, A.; de Marchi, M.; Masin, R. Can Commercial Low-Cost Drones and Open-Source GIS Technologies Be Suitable for Semi-Automatic Weed Mapping for Smart Farming? A Case Study in NE Italy. *Remote Sens.* **2021**, *13*, 1869. [CrossRef]
68. Rashid, K.J.; Hoque, M.A.; Esha, T.A.; Rahman, M.A.; Paul, A. Spatiotemporal Changes of Vegetation and Land Surface Temperature in the Refugee Camps and Its Surrounding Areas of Bangladesh after the Rohingya Influx from Myanmar. *Environ. Dev. Sustain.* **2021**, *23*, 3562–3577. [CrossRef]
69. Fitz, P.R.; Vieira, J.C.; Soares, M.C. The Use of Sampling Polygons in Supervised Classifications of Satellite Images. *Rev. Entre-Lugar* **2019**, *10*, 319–341. [CrossRef]
70. Ngubane, Z.; Odindi, J.; Mutanga, O.; Slotow, R. Assessment of the Contribution of WorldView-2 Strategically Positioned Bands in Bracken Fern (*Pteridium Aquilinum (L.) Kuhn*) Mapping. *S. Afr. J. Geomat.* **2014**, *3*, 210–223. [CrossRef]
71. Traganos, D.; Reinartz, P. Mapping Mediterranean Seagrasses with Sentinel-2 Imagery. *Mar. Pollut. Bull.* **2018**, *134*, 197–209. [CrossRef] [PubMed]
72. Karasiak, N.; Dejoux, J.F.; Fauvel, M.; Willm, J.; Monteil, C.; Sheeren, D. Statistical Stability and Spatial Instability in Mapping Forest Tree Species by Comparing 9 Years of Satellite Image Time Series. *Remote Sens.* **2019**, *11*, 2512. [CrossRef]
73. Congalton, R.G.; Green, K. *Assessing the Accuracy of Remotely Sensed Data: Principles and Practices*, 3rd ed.; CRC Press: Boca Raton, FL, USA, 2019; pp. 1–319. [CrossRef]

Disclaimer/Publisher's Note: The statements, opinions and data contained in all publications are solely those of the individual author(s) and contributor(s) and not of MDPI and/or the editor(s). MDPI and/or the editor(s) disclaim responsibility for any injury to people or property resulting from any ideas, methods, instructions or products referred to in the content.